pattern between 2011 and 2012, the northeast Bay of Bengal was saltier in 2013 than 2012, while the rest of the Bay of Bengal was fresher in 2013 than in 2012.

g. Surface currents—R. Lumpkin, G. Goni, and K. Dohan

This section describes ocean surface current changes, transports derived from ocean surface currents, and features such as rings inferred from surface currents. Surface currents are obtained from in situ (global array of drogued drifters and moorings) and satellite (altimetry, wind stress, and SST) observations. Transports are derived from a combination of sea height anomaly (from altimetry) and climatological hydrography. See previous *State of the Climate* reports, from 2011 and before, for details of these calculations. Anomalies are calculated with respect to the time period 1992–2007. Global zonal current anomalies and changes in anomalies from 2012 are shown in Fig. 3.17 and discussed below for individual ocean basins.

1) Pacific Ocean

Compared to the dramatic changes in 2012, 2013 was a relatively quiescent year in the tropical Pacific basin. It began with average January westward surface current anomalies of –25 to –30 cm s^{-1} (negative = westward) across the equatorial Pacific in the band 170°E–90°W, where the climatological westward speed is ~65 cm s^{-1}. By February, these equatorial anomalies had diminished dramatically and were present only in the longitude band 90°–150°W. Throughout the remainder of 2013, no large-scale equatorial anomalies persisted for more than a month.

The eastward North Equatorial Countercurrent (NECC) at 5°–8°N was ~10–20 cm s^{-1} faster than its climatological average from January until August. The longitude of anomalously fast NECC currents shifted westward through these months, located at 90°–140°W in January, 130°–160°W in June, and 130°W–180° in August. These anomalies weakened in September–October, and in November the NECC was close to its climatological strength across the basin.

In March, strong eastward anomalies of 20–30 cm s^{-1} developed at 2°S along 100°–150°W, where the climatological currents are near zero. The location of the anomalies propagated westward and diminished in magnitude through May, located at 150°W–180° in May when they were last seen.

The annual-average zonal current anomaly for 2013 in the Pacific (Fig. 3.17a) highlights the NECC anomalies at 5°–8°N that persisted through most of the year west of the dateline (see above). In the band 145°–170°E, anomalies of 15 cm s^{-1} at 20°N indicated a strengthening of the eastward Subtropical Countercurrent, while anomalies of –15 cm s^{-1} at 22°N corresponded to a strengthening of the westward flow located at this latitude. Alternating zonal bands of ~20 cm s^{-1} anomalies at 33°–36°N, 140°–160°E were consistent with a northward shift of the Kuroshio Extension from its annual climatological position, a shift seen since 2010. For the period 2010–13, the Kuroshio has exhibited a narrower and stronger annual mean signature, shifted approximately 1° in latitude to the north compared to 2006–09. While the climatological latitude of the Kuroshio core at 150°E is ~34.3°N, the core of the current in 2013 was at ~36.0°N, slightly south of the mean position during 2012 (36.7°N). The 2013 minus 2012 map (Fig. 3.17b) is dominated by the strong eastward anomalies that were present in February–August 2012 (Lumpkin et al. 2013).

Surface current anomalies in the equatorial Pacific typically lead SST anomalies by several months, with a magnitude that scales with the SST anomaly magnitude. Recovery to normal current conditions is also typically seen before SST returns to normal. Thus, current anomalies in this region are a valuable predictor of the evolution of SST anomalies and their related climate impacts. This leading nature can

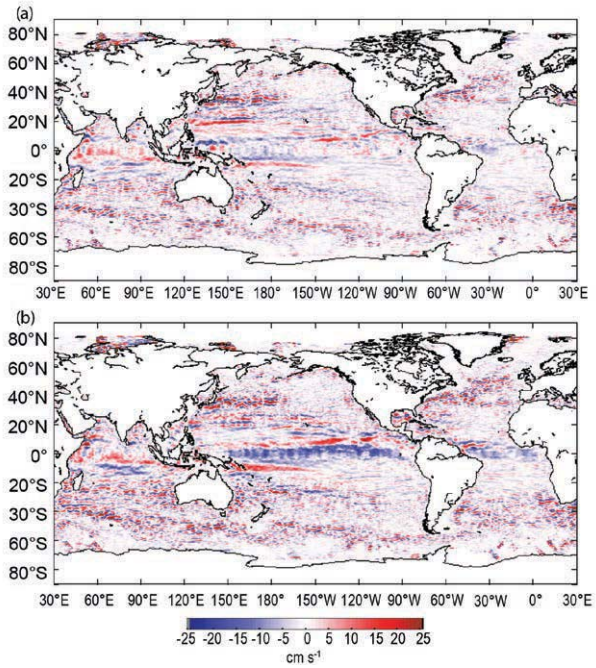

Fig. 3.17. Global zonal geostrophic anomalies for (a) 2013 and (b) 2013 minus 2012, in cm s^{-1}, derived from a synthesis of drifters, altimetry, and winds.

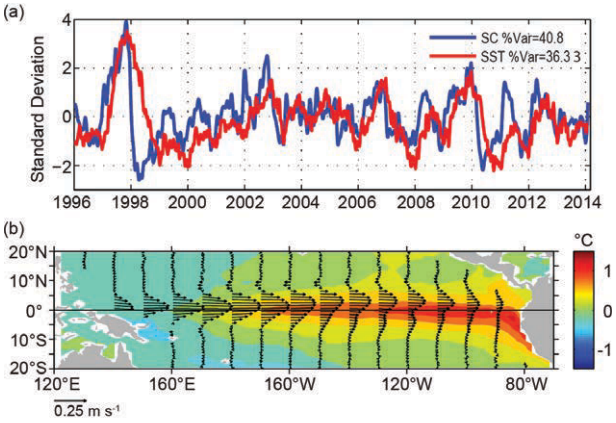

Fig. 3.18. Principal EOF of surface current (SC) and of SST anomaly variations in the tropical Pacific from the OSCAR model (Bonjean and Lagerloef 2002). (a) Amplitude time series of the EOFs normalized by their respective standard deviations for 1996 through 31 Jan 2014. (b) Spatial structures of the SC (vectors, m s^{-1}) and SST (color, °C) EOFs.

be seen in the first principal empirical orthogonal function (EOF) of surface current (SC) anomaly and separately of SST anomaly in the tropical Pacific basin (Fig. 3.18). In the period 1993–2013, the maximum correlation between SC and SST is $R = 0.70$ with SC leading SST by 76 days. Throughout 2013, this mode exhibited weak fluctuations around a slightly negative value for both SC and SST.

2) Indian Ocean

In the western equatorial Indian Ocean, the year began with ~20 cm s^{-1} eastward anomalies over the region 2°S–2°N, 40°–70°E. These anomalies were erased in February–March by the westward equatorial currents that develop during the northeast monsoon season (c.f., Beal et al. 2013). Eastward anomalies were also present in this region in August–November, although they were weaker and not as spatially coherent as in January. Outside this region, at scales larger than mesoscale, surface currents in the Indian Ocean were close to their climatological monthly values until May (i.e., after the northeast monsoon) when eastward anomalies of 15–30 cm s^{-1} developed at 60°–90°E, 2°S–1°N. The climatological May current in this band is 60 cm s^{-1} at 1°S. These anomalies weakened through June–July but remained present, and reintensified in August to 15–20 cm s^{-1}, extending as far south as 8°S in the same longitude band. In October, strong (–20 to –30 cm s^{-1}) westward anomalies appeared at 0°–3°N, 60°–90°E, erasing the pattern of eastward anomalies north of ~4°S (although eastward anomalies persisted at 4°–6°S). These westward anomalies persisted through November. By December, currents

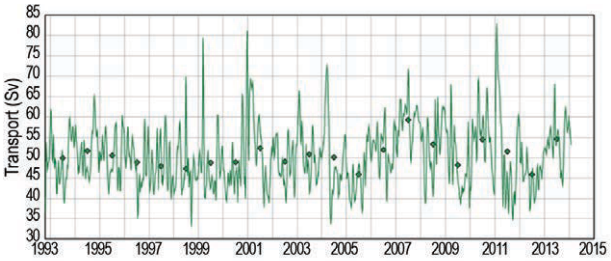

Fig. 3.19. Altimetry-derived transport of the Agulhas Current (Sv) from a combination of sea height anomaly and climatological hydrography. (Source: http://www.aoml.noaa.gov/phod/altimetry/cvar/agu/index.php.)

in the central Indian Ocean basin had returned to their climatological strengths.

The Agulhas Current transport is a key indicator of Indian-Atlantic ocean interbasin water exchanges (Goni et al. 1997). As noted in last year's report, the altimetry-derived annual mean transport of the Agulhas Current (Fig. 3.19) decreased abruptly in mid-2011 compared to its long-term (1993–2013) mean; this reduced transport persisted through 2012 but increased above the long-term average in 2013. In 2012, the annual mean Agulhas transport was ~46 Sv, which (along with 2005) was the lowest annual mean observed since the beginning of the altimetric record in 1993. This increased to an annual average of 54 Sv in 2013, a maximum surpassed only by one year (2007) in the record. Preliminary results indicate that five rings were shed during 2013, which is the average annual value.

3) Atlantic Ocean

In January 2013, currents in the central equatorial Atlantic (6°S–4°N, 5°–30°W) exhibited 10–20 cm s^{-1} eastward anomalies, reversing their direction from the climatological westward flow at ~5 cm s^{-1}. By February these anomalies were present in strength only at the latitude of the NECC, 5°–6°N, while they reduced to <10 cm s^{-1} elsewhere. Eastward anomalies persisted in the NECC until May. In August, westward equatorial anomalies developed across the basin, reaching –20 cm s^{-1} at 2°S in the longitude band 5°–35°W. These anomalies persisted in strength through September and weakened in October–November to ~10 cm s^{-1}, disappearing entirely by December.

During 2013, the velocity fields suggest that the annually-averaged Gulf Stream remained close to its climatological position. This is in contrast to 2012, when large-scale surface current anomalies indicated a northward shift of the Gulf Stream of 1°–1.5° latitude. The North Brazil Current (NBC), which sheds

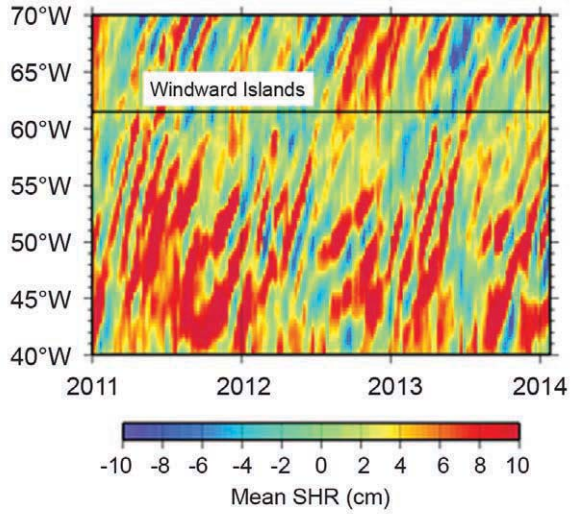

Fig. 3.20. Space-time diagram of de-seasoned sea height residual values (cm) along the NBC ring corridor during 2011–14. (Source: http://www.aoml.noaa.gov/phod/altimetry/cvar/nbc.)

rings that carry waters from the Southern Hemisphere into the North Atlantic basin, exhibited an annual transport close to climatology and shed eight rings, a larger-than-average value (Goni and Johns 2003). Sea height anomalies in the region, which have generally increased since 2001 (apart from the anomalous low years of 2003 and 2008), continued to exhibit higher-than-average values in 2013 (Fig. 3.20).

In the southwest Atlantic Ocean, the Brazil Current carries waters from subtropical to subpolar regions. The separation of the Brazil Current front from the continental shelf break continued to exhibit annual periodicity driven by wind stress curl variations (c.f., Goni and Wainer 2001). However, the annual mean separation of the front was at its average (1993–present) latitude after having exhibited extreme southward anomalies of up to 2° latitude during 2002–11 (http://www.aoml.noaa.gov/phod/altimetry/cvar/mal/BM_anm.php). That southward shift was related to a multidecadal oscillation or was in response to a secular trend in South Atlantic temperatures (c.f., Lumpkin and Garzoli 2010; Goni et al. 2011).

h. Meridional overturning circulation observations in the North Atlantic Ocean—M. O. Baringer, G. McCarthy, J. Willis, M. Lankhorst, D. A. Smeed, U. Send, D. Rayner, W. E. Johns, C. S. Meinen, S. A. Cunningham, T. O. Kanzow, E. Frajka-Williams, and J. Marotzke

The ocean's meridional overturning circulation (MOC) is the large-scale "conveyor belt" that redistributes heat, fresh water, carbon, and nutrients around the globe. Variability in the MOC dominates the variability of transported properties (not variability in the properties themselves), and so the discussion here is focused on the mean and variability of the MOC. For discussion of the importance of the MOC and the state of understanding of this the reader is referred to previous *State of the Climate* reports (e.g., Baringer et al. 2013) and recent reviews such as Macdonald and Baringer (2013), Lozier (2012), and Srokosz et al. (2012). This section reports the results provided by three MOC observing systems in the North Atlantic at 16°N, 26°N, and 41°N.

As part of the 26°N system, the Florida Current (FC, as the Gulf Stream is called at this latitude) has been measured since 1982. Measurements continued through 2013; however, the computer recording system failed twice, leading to two brief gaps in the time series during 28 October–4 November 2013 and during 15 December 2013–3 January 2014. The median transport (from 1982 to 2013) of the Florida Current is 32.0 ±0.26 Sv (standard error of the mean based on an integral time scale of about 20 days) with an insignificant downward trend of −0.25 ±0.28 Sv decade^{-1} (errors using 95% significance with a decorrelation time scale of about 20 days). In 2013 the annual median was 31.7 ±1.7 Sv with the annually-averaged transport essentially equivalent to the long-term average; the 2013 median is within the middle 50% of all annual averages. The daily FC transport values as compared to all previous years (Fig. 3.21a) indicate that 2013 was unusual in that there were several low transport values (extremes defined as outside the 95% confidence limits) during 8–14 March, 10–17 October, and early December. The lowest transport observed (19.7 Sv) occurred on 11 March. This low value was the ninth lowest transport recorded since 1982. During 2013 there was only one high transport event that exceeded the 95% confidence limits: during 10–12 June the transport reached 40.2 Sv.

The RAPID-MOC/MOCHA/WBTS 26°N mooring array continues to provide a twice-daily estimate of basin-wide MOC strength (Fig. 3.22) and is the most complete MOC existing observing system, measuring the full water column across the full basin and absolute transports in boundary currents (see Rayner et al. 2010 for details). McCarthy et al. (2012) noted statistically significant low MOC transport in the winter of 2009/10, showing that the low transport was predominantly caused by both a decrease in the northward Ekman transport and particularly by an increase in the southward interior transport: the overturning weakened as the gyre strengthened. Downturns in the overturning circulation such as